Electronic Supplementary Material (ESI) for Reaction Chemistry & Engineering.

Supporting Information

Reaction pathways and kinetics for tetra-alanine in hot, compressed liquid water

James D. Sheehan, Ashwin Abraham, and Phillip E. Savage

Department of Chemical Engineering, Pennsylvania State University, 119 Greenberg Complex, University Park, PA 16802, USA

Estimating Acid-Base Dissociation Constants of Alanine and Peptides

The enthalpies of reaction at 25 °C for the acid-base equilibrium reactions of alanine (Eq. 3 and 4) were estimated with the group additivity model developed by Amend and Helgeson.[1] This additivity model calculates the enthalpies of formation ($\Delta H_{f,AA}$) for each dissociation state of an amino acid by accounting for the contributions of the N- and C-termini or the "amino acid backbone", ($\Delta H_{f,AAB}$) and the R-group ($\Delta H_{f,R}$) to the molecular thermodynamic properties, as shown by Eq. S1.

$$\Delta H_{f,AA} = \Delta H_{f,AAB} + \Delta H_{f,R} \qquad (S1)$$

Eq. S2 was used in conjunction with the estimated enthalpies of formation for cationic, zwitterionic, and anionic forms of alanine for estimating the enthalpies of reaction. ΔG_{rxn} at 25 °C was calculated in a similar fashion using its analogous equation.

$$\Delta H_{rxn} = \sum_i \nu_i \, \Delta H_{f,i} \qquad (S2)$$

Similarly, the enthalpies of reaction at 25 °C for the acid-base equilibrium reactions of the alanine peptides were estimated with the group additivity model for unfolded proteins, also developed by Amend and Helgeson.[2] Briefly, the additivity model calculates the enthalpies of formation for zwitterionic alanine peptides ($\Delta H_{f,P}$) by accounting for the contributions of the N- and C-termini ($\Delta H_{f,AAB}$), peptide backbone ($\Delta H_{f,PB}$), and the R-groups ($\Delta H_{f,R_i}$) of the constituent amino acids to the thermodynamic properties, as shown by Eq. S3.

$$\Delta H_{f,P} = \Delta H_{f,AAB} + (n-1)\Delta H_{f,PB} + \sum_i n_i \, \Delta H_{f,R_i} \qquad (S3)$$

n is the number of constituent amino acids, and n_i is the number of R-group, i.

As values of $\Delta H_{f,AAB}$ related to the cationic and anionic states of peptides were not available, we estimated them from published enthalpies of reaction for the acid-base equilibrium reactions of di-glycine,[3,4] tri-glycine,[5] and tetra-glycine.[6] By joining Eq. S1 and S3 and using the reported enthalpies of reaction, the estimated enthalpy of formation for the zwitterionic state of the alanine peptides, and the appropriate values for $\Delta H_{f,PB}$, n, $\Delta H_{f,R_i}$, and n_i, we calculated

$\Delta H_{f,AAB}$ for the cationic and anionic states of the di-, tri-, and tetra-peptides. When calculating K_d at higher temperatures, we used the average values of $\Delta H_{f,AAB}$ for the cationic and anionic forms of di-, tri-, and tetra-peptides, -484.3 kJ/mol and -440.7 kJ/mol, respectively, as these varied little (i.e., standard deviations of ±0.4 kJ/mol and ±0.7 kJ/mol, respectively). We used the same approach for calculating the Gibbs free energies of reaction at 25 °C. The calculated thermodynamic quantities for the acid-base equilibrium reactions of alanine and alanine peptides are presented in Table 2.

Elucidating Reaction Pathways

We confirmed that alanine anhydride was a secondary product under basic conditions by analyzing a second-rank delplot. Figure S1 plots the selectivity divided by the conversion (i.e., yield divided by the conversion squared) vs. conversion. The y-intercept is clearly non-zero but finite, indicating that alanine anhydride is a secondary product of anionic tetra-alanine. The formation of alanine anhydride is likely from the cyclodehydration of di-alanine.

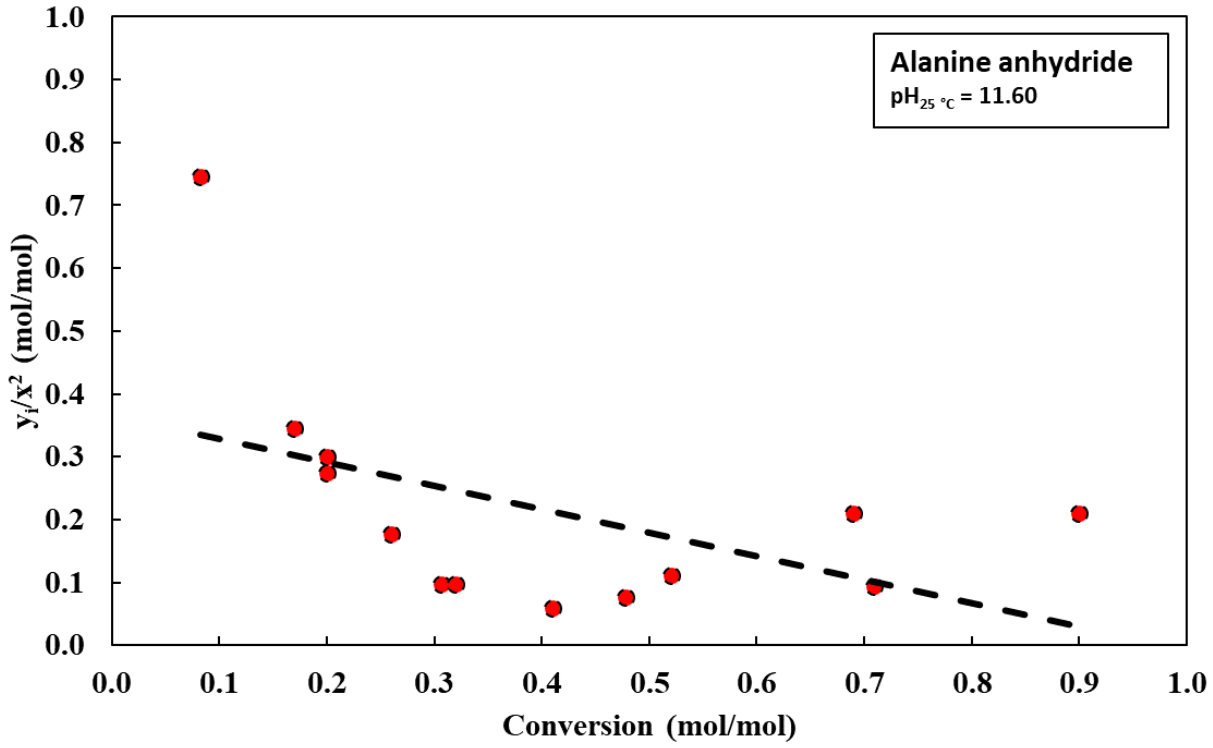

Figure S1: Second-rank delplot of alanine anhydride resulting from hydrothermal reactions of tetra-alanine solutions (170, 200, 230 °C) with initial pH of 11.60.

Evaluating Reaction Pathways and Model Selection Criteria

Three different models were investigated for correlating the experimental data. The models differentiated by incorporating different primary pathways for the zwitterionic tetra-alanine for producing alanine anhydride. Model 1 had both primary pathways for producing alanine anhydride, Model 2 had only the primary pathway leading exclusively to alanine anhydride (i.e., $k_3 = 0$), and Model 3 contained only the primary pathway leading to the formation of both di-alanine and alanine anhydride (i.e., $k_4 = 0$). The performances of the models were compared with the Akaike information criterion, as shown by Eq S4.

$$AIC = -2\,Log(L) + 2\,k \qquad (S4)$$

$Log(L)$ is the log-likelihood and k is the number of parameters.

The best performing model has the lowest AIC. However, AIC values are relative and the difference (Δ_i) between the AIC of a given model *i* (AIC_i) and the best performing model (AIC_{min}) allows for comparison. Further comparison of model performances can be quantified by the Akaike weight, as shown by Eq. S5.

$$w_i = \frac{e^{-0.5\,\Delta_i}}{\sum_j e^{-0.5\,\Delta_j}} \qquad (S5)$$

Briefly, w_i is the relative likelihood of model *i* divided by the sum of likelihoods of all proposed models. The collective sum of the Akaike weights equals 1 and larger w_i indicates stronger evidence supporting model *i*.

Table S1 provides the performance of the three proposed models. Model 3 resulted with AIC and Akaike weight that demonstrated its superior ability in modeling the experimental data. This modeling comparison suggests that only a single primary reaction pathway from zwitterionic tetra-alanine leads to the formation of alanine anhydride. Thus, in the subsequent sections we provide results of model 3 which includes a pathway from zwitterionic tetra-alanine to alanine anhydride and di-alanine and no pathway to solely alanine anhydride (i.e., $k_4 = 0$).

Table S1: Statistics and selection criteria for proposed models.

Model	Parameters	-2 log(L)	AIC_i	Δ_i	w_i
Model 1	20	-5020	-4979	104	0.00
Model 2 ($k_3 = 0$)	20	-5023	-4982	101	0.00
Model 3 ($k_4 = 0$)	20	-5123	-5083	0	1.00

Supplementary Tables and Figures

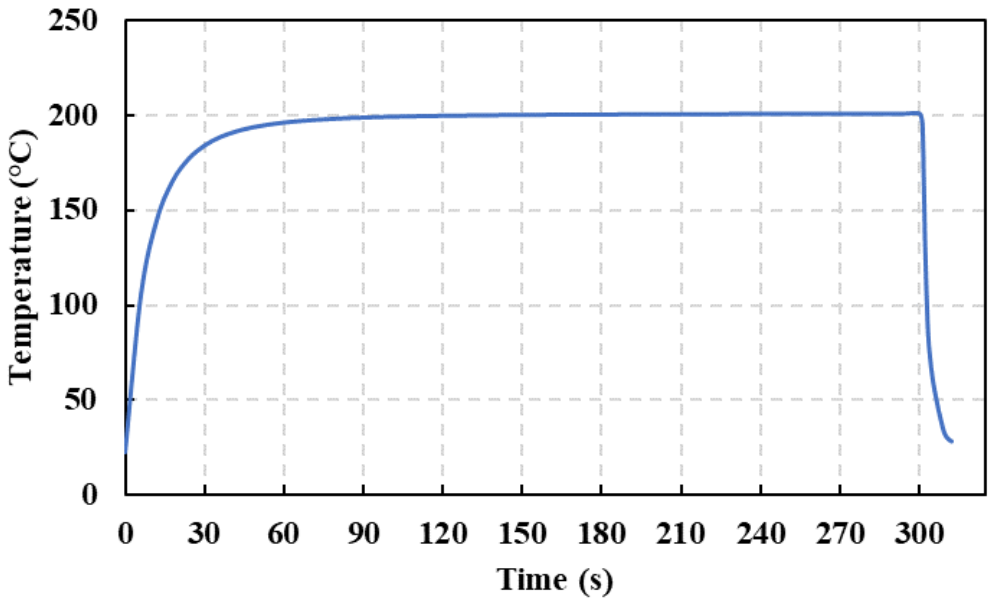

Figure S2: Temperature profile of batch reactor heating to 200 °C and quenching to room temperature.

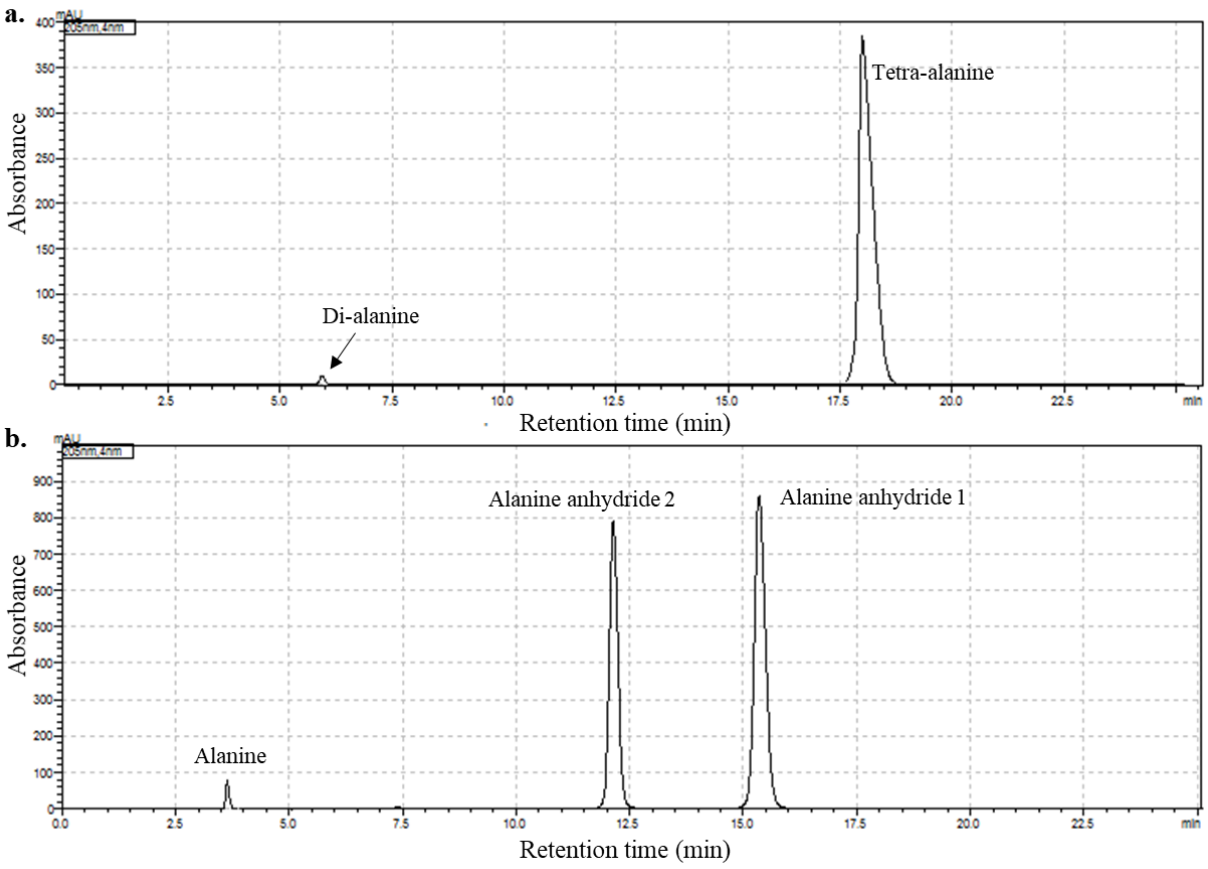

Figure S3: HPLC chromatogram of samples collected from hydrothermal reaction of tetra-alanine (initial concentration of 4 mM at ambient conditions) at 200 °C for 0 min (a.) and 60 min (b.).

Table S2: Conversion of tetra-L-alanine and yields of tetra-alanine (Ala_4), tri-alanine (Ala_3), di-alanine (Ala_2), alanine anhydride ($Ala_{2,\ anhydride}$), alanine (Ala_1), and the balance (i.e., the sum of yields) resulting from reaction in subcritical water at 170 °C, 200 °C, and 230 °C, at varying batch holding times and initial pH. Concentrations of tetra-alanine feedstock were 4 mM.

Temperature (°C)	pH_{feed}	Time (min)	Conversion of Ala_4 (mol/mol)	Ala_3 (mol/mol)	Ala_2 (mol/mol)	$Ala_{2,\ anhydride}$ (mol/mol)	Ala_1 (mol/mol)	Balance
170	3.30	0	0.00±0.00	0.00±0.00	0.00±0.00	0.00±0.00	0.00±0.00	1.00±0.00
		15	0.03±0.00	0.01±0.00	0.03±0.00	0.00±0.00	0.02±0.00	1.02±0.01
		30	0.21±0.03	0.00±0.00	0.03±0.00	0.07±0.01	0.02±0.00	0.92±0.04
		60	0.54±0.00	0.00±0.00	0.03±0.00	0.21±0.01	0.05±0.00	0.75±0.01
		90	0.68±0.02	0.00±0.00	0.03±0.00	0.43±0.02	0.10±0.01	0.89±0.05
	5.65	0	0.00±0.00	0.00±0.00	0.00±0.00	0.00±0.00	0.00±0.00	1.00±0.00
		15	0.10±0.05	0.00±0.00	0.05±0.00	0.08±0.00	0.02±0.00	1.06±0.05

		30	0.39±0.01	0.00±0.00	0.08±0.00	0.19±0.01	0.05±0.00	0.92±0.03
		60	0.55±0.02	0.00±0.00	0.08±0.00	0.32±0.02	0.08±0.00	0.93±0.04
		90	0.63±0.02	0.00±0.00	0.09±0.01	0.43±0.01	0.11±0.00	1.00±0.05
	11.60	0	0.00	0.00	0.00	0.00	0.00	1.00
		10	0.17±0.03	0.03±0.00	0.03±0.00	0.00±0.00	0.01±0.00	0.90±0.03
		15	0.20	0.04	0.02	0.00	0.01	0.88
		30	0.26±0.06	0.09±0.00	0.05±0.00	0.00±0.00	0.03±0.00	0.92±0.07
		60	0.20	0.09	0.05	0.00	0.03	0.98
		90	0.41±0.04	0.18±0.00	0.12±0.00	0.01±0.00	0.10±0.00	1.00±0.05
200	3.30	0	0.01±0.01	0.00±0.00	0.01±0.00	0.00±0.00	0.00±0.00	1.00±0.01
		5	0.32±0.04	0.00±0.00	0.03±0.00	0.14±0.00	0.03±0.00	0.89±0.04
		15	0.61±0.00	0.00±0.00	0.02±0.00	0.37±0.02	0.09±0.00	0.87±0.02
		30	0.77±0.00	0.00±0.00	0.02±0.00	0.61±0.02	0.17±0.00	1.04±0.02
		60	0.96±0.00	0.00±0.00	0.02±0.00	0.71±0.00	0.20±0.01	0.97±0.02
	5.65	0	0.05±0.04	0.00±0.00	0.01±0.00	0.00±0.00	0.00±0.00	0.97±0.04
		5	0.42±0.03	0.00±0.00	0.06±0.00	0.17±0.00	0.04±0.00	0.85±0.03
		15	0.76±0.00	0.00±0.00	0.05±0.00	0.41±0.00	0.10±0.00	0.80±0.01
		30	0.86±0.10	0.00±0.00	0.04±0.00	0.51±0.10	0.13±0.04	0.82±0.03
		60	1.00±0.00	0.00±0.00	0.02±0.00	0.70±0.00	0.21±0.00	0.92±0.01
	11.60	0	0.00±0.02	0.01±0.00	0.00±0.00	0.00±0.00	0.00±0.00	1.01±0.02
		5	0.08±0.02	0.06±0.00	0.02±0.00	0.01±0.00	0.02±0.00	1.03±0.03
		15	0.31±0.01	0.13±0.00	0.06±0.00	0.01±0.00	0.06±0.00	0.94±0.02
		30	0.48±0.00	0.18±0.01	0.10±0.00	0.02±0.00	0.11±0.00	0.93±0.01
		60	0.71±0.06	0.15±0.01	0.15±0.01	0.05±0.00	0.18±0.01	0.83±0.08
230	3.30	0	0.06±0.01	0.00±0.00	0.02±0.00	0.04±0.01	0.00±0.00	1.00±0.00
		5	0.77±0.02	0.00±0.00	0.01±0.00	0.50±0.02	0.13±0.00	0.88±0.00
		10	0.95±0.00	0.00±0.00	0.01±0.00	0.64±0.00	0.17±0.00	0.87±0.00
		15	0.99±0.00	0.00±0.00	0.01±0.00	0.74±0.04	0.21±0.01	0.97±0.06
		30	1.00±0.00	0.00±0.00	0.01±0.00	0.70±0.02	0.20±0.01	0.91±0.04
	5.65	0	0.18	0.00	0.05	0.10	0.03	1.00
		10	1.00±0.00	0.00±0.00	0.03±0.00	0.67±0.00	0.19±0.00	0.89±0.01
		15	1.00±0.00	0.00±0.00	0.03±0.01	0.74±0.02	0.22±0.00	0.99±0.02
		30	1.00±0.00	0.00±0.00	0.01±0.00	0.62±0.01	0.20±0.00	0.84±0.01
		45	1.00±0.00	0.00±0.00	0.01±0.00	0.68±0.01	0.23±0.01	0.92±0.02

11.60	0	0.03	0.03	0.01	0.00	0.00	1.00
	5	0.32±0.00	0.15±0.00	0.06±0.00	0.01±0.00	0.06±0.01	0.97±0.01
	10	0.52±0.03	0.19±0.00	0.10±0.00	0.03±0.00	0.12±0.00	0.91±0.03
	15	0.69±0.06	0.13±0.02	0.15±0.04	0.10±0.06	0.19±0.03	0.88±0.16
	30	0.90±0.01	0.04±0.01	0.16±0.02	0.17±0.01	0.30±0.00	0.77±0.04

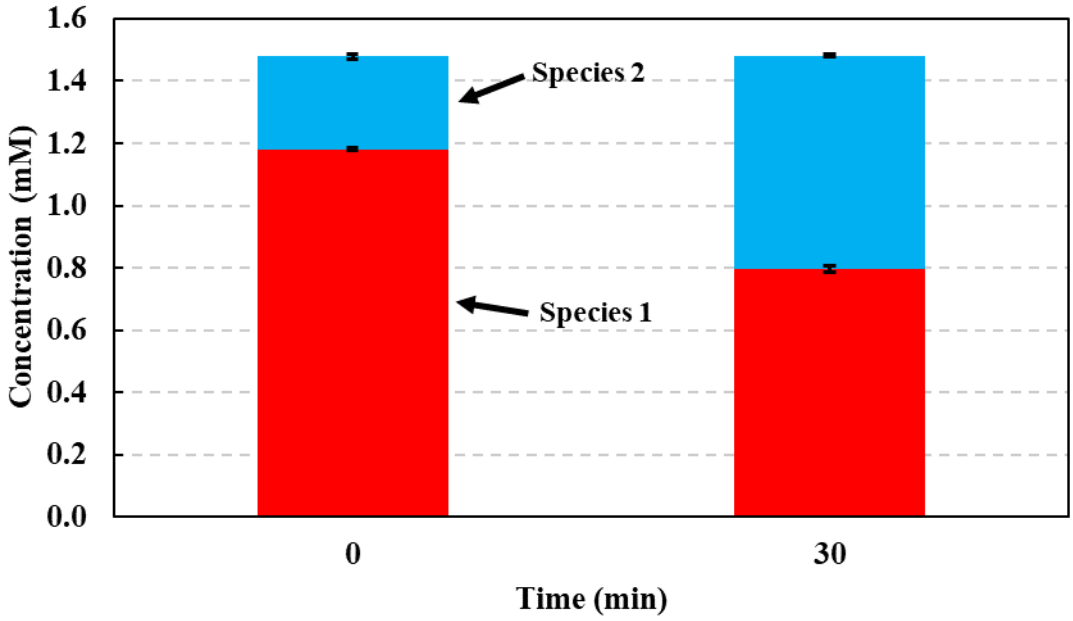

Figure S4: Reaction of alanine anhydride (initial concentration of 1.5 mM) at 230 °C for 0 min and 30 min. Species 1 is the original species within the prepared feedstock loaded into the batch reactors. The mass balance of near unity between the experimental conditions signifies no ring opening of alanine anhydride and that Species 2 likely forms from the direct racemization of a chirality center in Species 1. Presence of Species 2 at 0 min indicates that racemization of Species 1 begins to occur during heat up of the batch reactor.

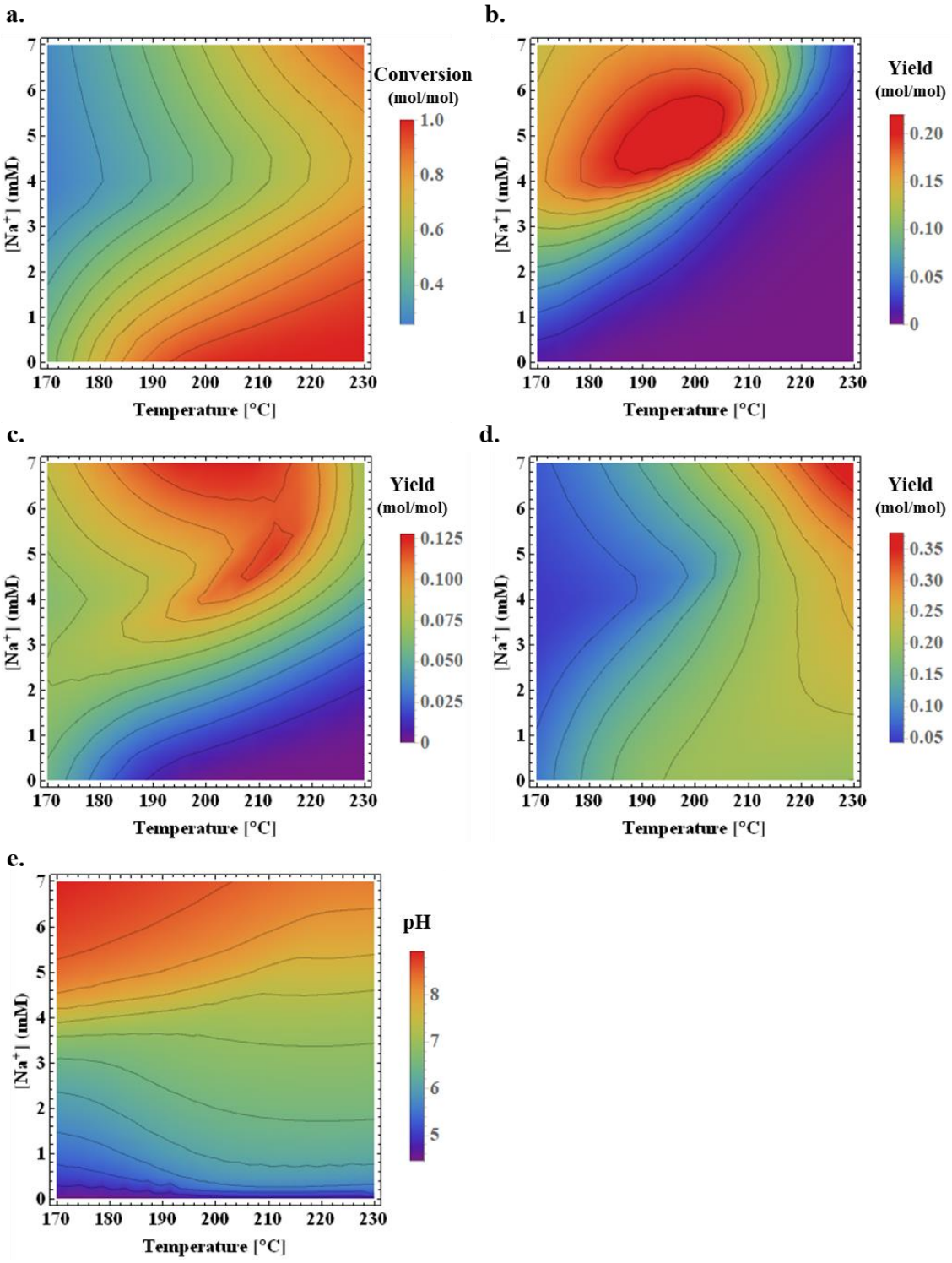

Figure S5: Predicted conversion of tetra-alanine (a.), yield of tri-alanine (b.), di-alanine (c.), alanine (d.), and pH of the reaction medium (e.), as functions of the concentration of sodium cation (from added NaOH) and temperature, resulting from the hydrothermal reaction of 3.5 mM tetra-alanine for 60 min. Contours indicate constant values.

References

1. Amend JP, Helgeson HC. Calculation of the standard molal thermodynamic properties of aqueous biomolecules at elevated temperatures and pressures Part 1L-α-Amino acids. J Chem Soc Faraday Trans. 1997;93(10):1927–41.
2. Amend JP, Helgeson HC. Calculation of the standard molal thermodynamic properties of aqueous biomolecules at elevated temperatures and pressures II. Unfolded proteins. Biophys Chem. 2000;84(2):105–36.
3. King EJ. The Thermodynamics of Ionization of Amino Acids. IV. The First Ionization Constants of Some Glycine Peptides. J Am Chem Soc. 1956;78(23):6020–4.
4. King EJ. Thermodynamics of Ionization of Amino Acids Part 6. The Second Ionization Constant of Some Glycine Peptides. J Am Chem Soc. 1975;79(6154):88–96.
5. Brunetti AP, Lim MC, Nancollas GH. Thermodynamics of Ion Association. XVII. Copper Complexes of Diglycine and Triglycine. J Am Chem Soc. 1968;90(19):5120–6.
6. Nancollas GH, Poulton DJ. Thermodynamics of ion association. XVIII. Copper complexes of tetraglycine. Inorg Chem. 1969;8(3):680–2.